Ω

SPE 36514

Hierarchical Object-Based Geostatistical Modeling of Fluvial Reservoirs

C.V. Deutsch, SPE, and L. Wang, Stanford U.

Abstract

This paper presents a novel approach to modeling braided stream fluvial reservoirs. The approach is based on a hierarchical set of coordinate transformations involving relative stratigraphic coordinates, translations, rotations, and straightening functions. The emphasis is placed on geologically-sound geometric concepts and realistically attainable conditioning statistics including areal and vertical facies proportions. The equations for the eight-fold coordinate transformation, a new analytical channel cross section shape, and a real example with 20 wells are presented.

Introduction

A characteristic feature of many fluvial reservoirs is the presence of sinuous sand-filled channels within a background of floodplain shale. Techniques for realistically modeling the spatial distribution of channels are necessary for reliable volumetrics, connectivity assessment, and input to flow simulation. The approach presented here is applicable to stochastic modeling channel shapes and filling those shapes with porosity and permeability.

Modeling proceeds sequentially[1,2]. Each major stratigraphic layer is modeled independently. The channel complex distribution, within a layer-specific stratigraphic coordinate system, is established first. Then, within each channel complex, the distribution of individual channels is simulated using appropriate transformed coordinate systems. This process is repeated down the hierarchy of geological units until the desired level of detail has been achieved. Finally, at the last coordinate system, petrophysical properties such as porosity and permeability are simulated with cell-based geostatistical algorithms within each facies.

This paper addresses the stochastic modeling of channel complexes and channels within a major reservoir layer. Multiple reservoir layers would be successively modeled and combined in a single reservoir model for volumetrics and flow simulation. At a higher level of iteration, multiple stochastic reservoir models could be constructed for assessing uncertainty.

An important feature of any approach to reservoir modeling is data conditioning. The data considered in this paper include lithofacies, porosity, and permeability data from wells, size and shape parameters of channel complexes, size and shape parameters of individual channels, vertical facies proportion curves, and areal facies proportion maps.

The approach presented in this paper has been inspired by the clear geometries observed at outcrops and as viewed from airplane windows in modern fluvial settings. There are similar object-based approaches documented in the literature[3,4,5,6,7,8]. The approach adopted here is distinct from conventional object-based fluvial reservoir modeling in a number of ways, (1) the use of an explicit reversable hierarchy of coordinate transformations that is keyed to sound sequence stratigraphic concepts[9], (2) geologically-intuitive and accessible input data controlling channel sizes and shapes, (3) explicit control over vertically varying and areally varying facies proportions, (4) realistic asymmetric channel geometries, (5) realistic non-undulating channel top surfaces, and (6) integrated porosity and permeability models where the main directions of continuity conform to channel geometries.

Coordinate Systems

The key to geometric object-based modeling is adapting the coordinate system to the appropriate principal directions of continuity. The direction of continuity depends on the scale of observation and the specific geological feature being modeled. Table 1 summarizes eight coordinate transformations from the largest scale to the smallest. Note the self similarity of coordinate transformations between channel complexes and individual channels. The initial reservoir coordinate system (x_1, y_1, z_1) may be any arbitrary system of two areal coordinates and an elevation coordinate.

No. 1: Vertical Transform to Stratigraphic Coordinates

Each major stratigraphic layer is modeled independently. The first step is to define a layer-specific relative stratigraphic coordinate from four structural grids: (1) the existing top z_{et}, (2) the existing base z_{eb}, (3) the restored top z_{rt}, and (4) the restored base z_{rb}. As shown on Fig. 1, the restored grids allow calculation of the stratigraphic coordinate as:

$$Z_2 = \frac{Z_1 - Z_{rb}}{Z_{rt} - Z_{rb}} \tag{1}$$

where z_2 is the stratigraphic vertical coordinate and z_1 is the elevation of the data location. The coordinate z_2 is 0 at the stratigraphic (restored) base and 1 at the stratigraphic top and thus represents a relative time coordinate. Subsequent modeling considers z_2 as the vertical coordinate. This transform may be reversed by:

$$Z_1 = Z_{rb} + Z_2(Z_{rt} - Z_{rb}) \tag{2}$$

Any back-transformed z_1 value outside of the interval $[z_{eb}, z_{et}]$ is not kept in the final model.

Faulted reservoirs must first be *unfaulted* by reversing the offset at each fault location. Left unchanged, faults may lead to the four grids being undefined at some locations and equivocally defined at other locations.

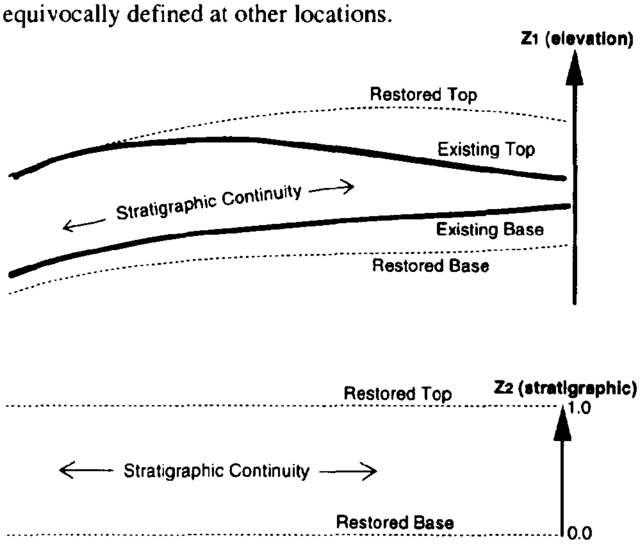

Figure. 1: Coordinate transformation from the original depth coordinate z_1 to stratigraphic vertical coordinate z_2.

No. 2: Areal Translation and Rotation

The *reservoir* coordinate system is based on an arbitrary east x_1 and north y_1 coordinate system (perhaps UTM coordinates). An areal translation and rotation is carried out to obtain a coordinate system with a *stratigraphic* y_2 aligned with the principal paleoslope direction, that is, the direction that, on average, has the greatest continuity. The *stratigraphic* x_2 is perpendicular to y_2, and most often corresponds to the direction of least continuity.

Fig. 2 illustrates the relationship between the two coordinate systems. Algebraically, they are related by the relations:

$$\begin{bmatrix} x_2 \\ y_2 \end{bmatrix} = \begin{bmatrix} \cos\theta & -\sin\theta \\ \sin\theta & \cos\theta \end{bmatrix} \begin{bmatrix} x_1 - x_1^0 \\ y_1 - y_1^0 \end{bmatrix} \tag{3}$$

and

$$\begin{bmatrix} x_1 \\ y_1 \end{bmatrix} = \begin{bmatrix} \cos\theta & \sin\theta \\ -\sin\theta & \cos\theta \end{bmatrix} \begin{bmatrix} x_2 \\ y_2 \end{bmatrix} + \begin{bmatrix} x_1^0 \\ y_1^0 \end{bmatrix} \tag{4}$$

where (x_1^0, y_1^0) is the location of the origin of the stratigraphic coordinate system in units of the original coordinate system, and θ is the rotation angle defined clockwise from the north direction y_1.

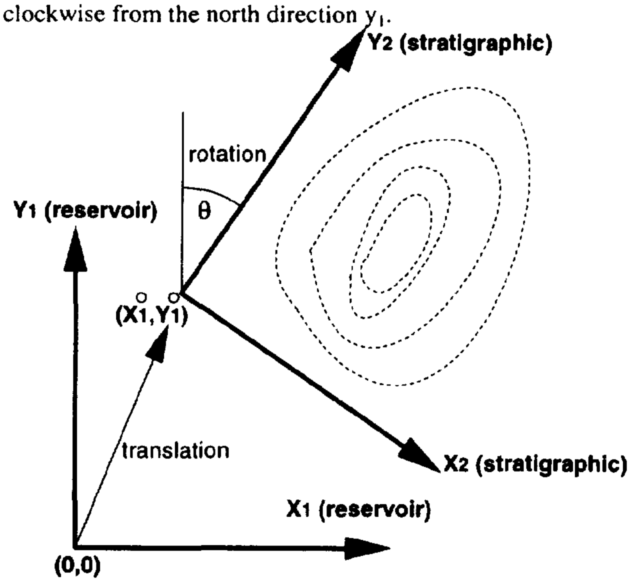

Figure. 2: Areal transform (translation and rotation) from reservoir to stratigraphic coordinate systems.

No. 3: Channel Complex Translation and Rotation

Fluvial channels often cluster together in *channel complexes*, also called *channel belts*. A single large channel complex may be used to handle the case where all individual channels are uniformly dispersed throughout the stratigraphic layer.

Fig. 3 illustrates the channel complex direction (ccd) in the areal stratigraphic coordinate space (x_2, y_2). A second areal translation and rotation is carried out to obtain a coordinate system with a ccd direction y_3 different from the predominant paleoslope direction (y_2) by an angle α, a direction x_3 perpendicular to ccd, and an origin at (x_2^s, 0). The (x_2, y_2) and (x_3, y_3) coordinate systems are related by relations:

$$\begin{bmatrix} x_3 \\ y_3 \end{bmatrix} = \begin{bmatrix} \cos\theta & -\sin\theta \\ \sin\theta & \cos\theta \end{bmatrix} \begin{bmatrix} x_2 - x_2^s \\ y_2 \end{bmatrix} \tag{5}$$

and

$$\begin{bmatrix} x_2 \\ y_2 \end{bmatrix} = \begin{bmatrix} \cos\theta & \sin\theta \\ -\sin\theta & \cos\theta \end{bmatrix} \begin{bmatrix} x_3 \\ y_3 \end{bmatrix} + \begin{bmatrix} x_2^s \\ 0 \end{bmatrix} \tag{6}$$

where α is the rotation angle defined clockwise from paleoslope direction y_2.

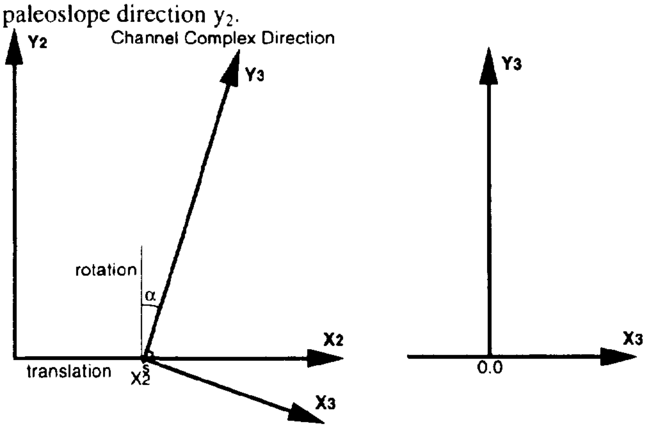

Figure 3: Channel Complex Direction (ccd) line and coordinate system.

Corrected Width

For consistency with previous coordinate systems, the width of a channel complex is measured perpendicular to the y_3 coordinate direction. This causes the effective width of the channel complex to be too narrow when not aligned with the y_3 axis. The following correction is proposed to increase the apparent width $W_a(y)$ so that the effective width is constant:

$$W_a(y) = W(y)/\cos(\beta(y)) \tag{7}$$

where $\beta(y)$ is the angle between the y-coordinate and the local tangent to the channel center line. Note that $W_a(y)$, is only defined for the interval $-90<\beta<90$. In other words, the channels are not allowed to "roll over". This is not considered a limitation for braided stream environments.

No. 4: Channel Complex Straightening

The center line of the channel complex undulates along the channel complex direction (ccd). Fig. 4 shows the channel complex center line and the dashed lines that represent the channel areal limits. A piecewise linear function $f^{cc}(y_3)$ measures the deviation of the channel complex center line from the channel complex direction (ccd). A "straight" horizontal coordinate x_4 is then defined as the horizontal deviation from the channel complex center line:

$$x_4 = x_3 - f^{cc}(y_3) \tag{8}$$

This transform is reversed as:

$$x_3 = x_4 + f^{cc}(y_3) \tag{9}$$

The y and z coordinates are left unchanged.

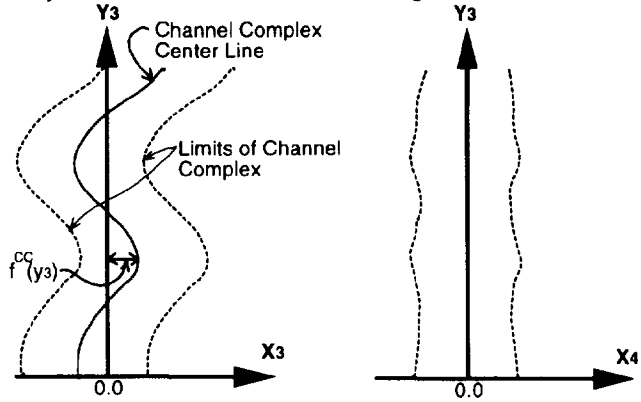

Figure 4: Transformation from the channel complex direction to a channel complex coordinates system following the sinuous channel complex center line

No. 5: Relative Channel Complex Coordinate

A relative horizontal coordinate x_5 is defined to make the channel complex boundaries parallel along y_3:

$$x_5 = \frac{2}{W_a(y_3)} x_4 \tag{10}$$

This transform is reversed as:

$$x_4 = \frac{W_a(y_3)}{2} x_5 \tag{11}$$

Once again, the y_3 and z coordinates are left unchanged. Fig. 5 illustrates this operation.

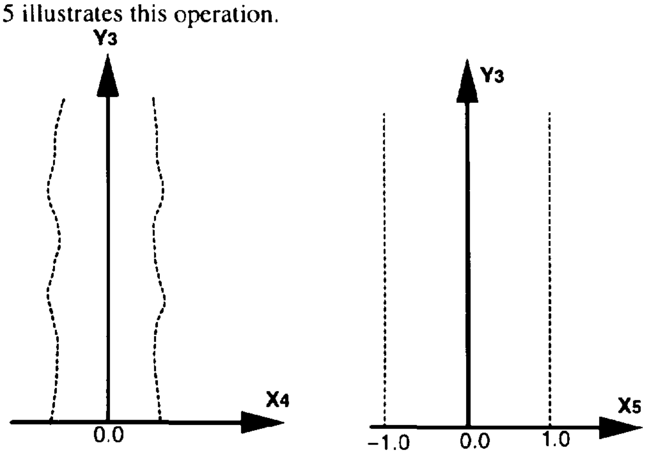

Figure 5: Transformation from channel complex coordinate system to relative channel complex coordinates

No. 6: Channel Translation

A single translation is required to position a channel direction line within the channel complex. The new coordinate system (x_6,y_3) is related to the previous coordinate system (x_5,y_3) by:

$$\begin{bmatrix} x_6 \\ y_3 \end{bmatrix} = \begin{bmatrix} 1 & 0 \\ 0 & 1 \end{bmatrix} \begin{bmatrix} x_5 - x_5^s \\ y_3 \end{bmatrix} \tag{12}$$

and

$$\begin{bmatrix} x_5 \\ y_3 \end{bmatrix} = \begin{bmatrix} 1 & 0 \\ 0 & 1 \end{bmatrix} \begin{bmatrix} x_6 \\ y_3 \end{bmatrix} + \begin{bmatrix} x_5^s \\ 0 \end{bmatrix} \tag{13}$$

Fig. 6 illustrates this operation.

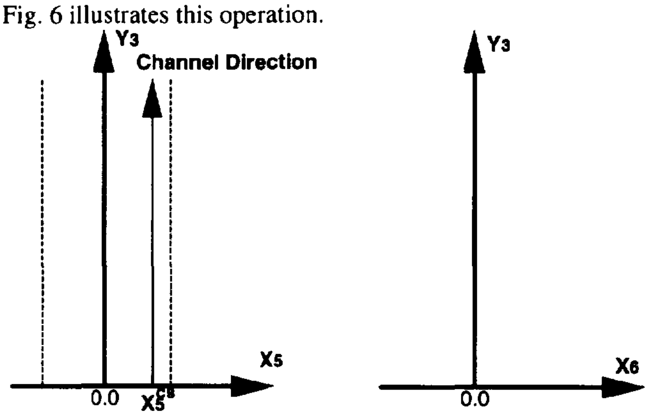

Figure 6: The individual channel direction coordinate system is obtained by translation from the channel complex direction.

No. 7: Channel Straightening

The center line of each channel undulates along the channel direction, see Fig. 7. A piecewise linear function $f^c(y_3)$ measures the deviation of the channel center line from the channel direction. A "straight" horizontal coordinate x_7 is then defined as the horizontal deviation from the channel center line:

$$x_7 = x_6 - f^c(y_3) \tag{14}$$

This transform is reversed as:

$$x_6 = x_7 + f^c(y_3) \tag{15}$$

The y and z coordinates are left unchanged.

No. 8: Relative Channel Coordinate

As was done for the channel complex in No. 5, a relative horizontal coordinate x_8 is defined to make the channel boundaries parallel, see Fig. 8:

$$x_8 = \frac{2}{W_a^c(y_3)} x_7 \tag{16}$$

This transform is reversed as:

$$x_7 = \frac{W_a^c(y_3)}{2} x_8 \tag{17}$$

A regular Cartesian coordinate system (x_8, y_3, z_2) is now achieved within which the variability of the petrophysical properties can be modeled with conventional techniques[10,11].

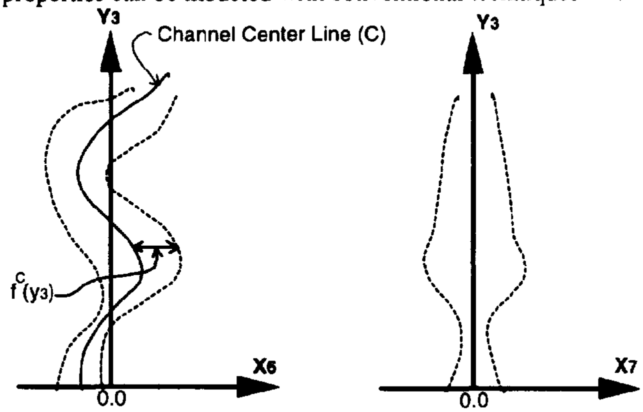

Figure 7: Transformation from the channel direction to a channel coordinate system following the sinuous channel center line.

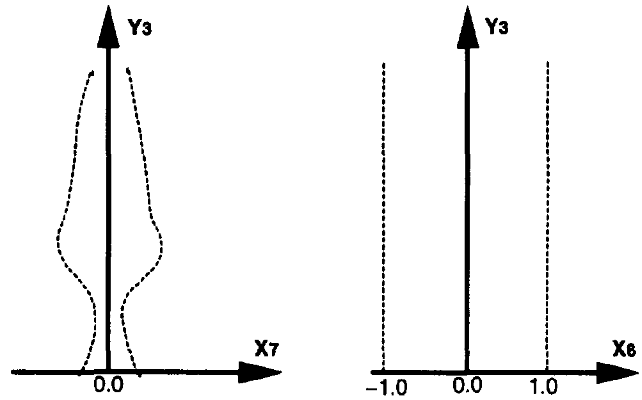

Figure 8: Transformation from channel coordinate system to relative channel coordinate system (between left bank and right bank) for modeling petrophysical properties such as porosity and permeability.

Channel Geometry and Construction

The geometry of each channel is defined by size parameters, location parameters, and 1-D functions; namely, a center line coordinate, width, thickness, and the relative position of maximum thickness between the channel banks, see Figure 10. The relative position of maximum thickness depends on the channel curvature (first subsection below). Analytical expressions for the position of maximum thickness and the channel cross section geometry are presented in the second and third subsections below.

Channel Curvature

The local curvature $C_v(y)$ of each channel center line is required to define the channel cross section geometry. As shown on Fig. 9, the curvature of a line $C_v(y)$ is calculated as:

$$C_v(y) = \frac{1}{\rho} = \lim_{AB \to 0} \frac{\theta}{AB} \tag{18}$$

where ρ is the radius of curvature, θ is the angle defined by the counter-clockwise rotation going from the tangent at B to the tangent at A, and AB is the length of arc from A to B.

The actual calculation of $C_v(y)$ in a discrete setting is illustrated in Fig.9.b. The local curvature at node T_i can be calculated by the angle between tangents at T_i and T_{i+1} divided by the length of arc $T_i\ T_{i+1}$ approximated by the following:

$$T_iT_{i+1} = \sqrt{1 + \left(x_{T_{i+1}} - x_{T_i}\right)^2} \tag{19}$$

The angle between y-axis and tangent at node T_i can be approximated by:

$$\theta_{T_i} = \tan^{-1}\left(x_{T_{i+1}} - x_{T_i}\right) \tag{20}$$

Similarly, at node T_{i+1},

$$\theta_{T_{i+1}} = \tan^{-1}\left(x_{T_{i+2}} - x_{T_{i+1}}\right) \tag{21}$$

Then, the local curvature at node T_i is calculated as:

$$C_v\left(y_{T_i}\right) = \frac{\theta_{T_{i+1}} - \theta_{T_i}}{T_iT_{i+1}} \tag{22}$$

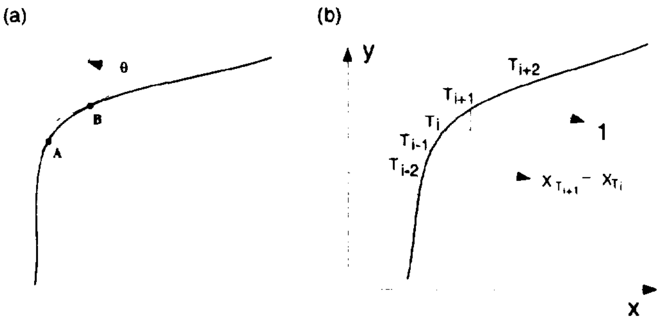

Figure 9: Curvature calculation along channel centerline.

Position of Maximum Thickness

The asymmetric channel cross section is modeled with the position of maximum thickness closer to the outside bank of the channel. A deterministic positioning is proposed below; a stochastic assignment could be considered with supporting outcrop or modern analogue data.

The first step is to scan through the entire centerline and calculate the local curvature $C_v(y)$. Denote the maximum absolute value of $C_v(y)$ of both signs (right and left), denoted as $C^r_v(y)$ and $C^l_v(y)$. The relative position a(y) of maximum thickness along the channel width is calculated as:

$$a(y) = \begin{cases} \dfrac{W(y)}{2}\left(1 - \dfrac{\left|C_v(y)\right|}{C^l_v}\right) & C_v(y) < 0 \\ \dfrac{W(y)}{2} & C_v(y) = 0 \\ \dfrac{W(y)}{2}\left(1 + \dfrac{\left|C_v(y)\right|}{C^r_v}\right) & C_v(y) > 0 \end{cases} \tag{23}$$

Channel Cross Section Geometry

Each sand-filled channel is geometrically defined by a channel width W(y), maximum thickness t(y), and the relative position a(y) of the maximum thickness, see Figure 10. The equation for the depth of the channel base below the channel top when a(y) < 0.5 (maximum thickness closer to the left bank) is:

$$d(w,y) = 4t(y)\left(\frac{w}{W(y)}\right)^{b(y)}\left[1 - \left(\frac{w}{W(y)}\right)^{b(y)}\right] \tag{24}$$

where b(y) = -Ln((2) / (a(y)), and $w \in [0, W(y)]$.

When a(y) > 0.5 (maximum thickness closer to the right bank as in Fig. 10 the depth of the channel base below the channel top is given by:

$$d(w,y) = 4t(y)\left(1 - \left(\frac{w}{W(y)}\right)\right)^{c(y)}\left[1 - \left(1 - \frac{w}{W(y)}\right)^{c(y)}\right] \tag{25}$$

where c(y) = -Ln((2) / (1-a(y)).

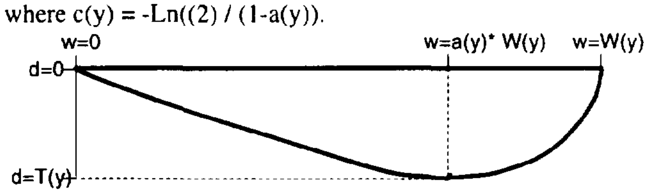

Figure 10: Vertical section of the channel geometry.

In the proposed simulation procedure, W(y) is simulated and a(y) is made a deterministic function of the local curvature of a simulated channel center line. The function d(w,y) defined by formulas 24 and 25 is symmetric at a(y)=0.5.

The cross-section areal size at a given y coordinate may be calculated analytically by integrating equation 24 and 25. One finds that the cross sectional areal is between 0.4 and 0.65 times W(y) t(y)

A 3-D channel is constructed as a horizontally elongated stack of 2-D cross sections along the y-coordinate direction. The shapes of these stacks along the y direction are determined by the parameters W(y) and a(y) simulated from smoothly varying stochastic fields. Each channel is filled with porosity and permeability using the appropriate within-channel coordinate system. The vertical coordinate system could be take parallel to the top channel surface or proportional between the top and base surfaces. Onlap correlation, where the correlation parallels the channel top, has been used in this paper. The base of each channel may have shale clasts or basal deposits that lower porosity and, more importantly, permeability. Furthermore, there may be a systematic trend in porosity from the base to the top of each channel. These features could be handled easily, since the position of each channel base is known, by a trend in the porosity modeling program.

Geological Conditioning Data

The approach documented in this paper aims at simulating a distribution of channels within a reservoir strata bounded by chronostratigraphic surfaces[9]. These surfaces are provided through well and seismic data, possibly with the aid of a mapping algorithm.

In practice, most geometric data inputs for channel modeling will be difficult to infer from available well and seismic data. It may then be necessary to adapt measurements from analogue outcrops, modern depositional systems, and similar densely drilled fields.

Facies Proportions

The proportion of channel sand may be specified by a vertical proportion curve, an areal proportion map, and a reference global proportion. The reference global proportions are denoted as P^k_g, k=1,...,K, where K is the number of facies. A vertical proportion curve specifies the proportion of a facies k as a function of vertical elevation or time and is denoted as P^k_v (z) where z ∈ (0,1]. Areal proportion maps specify the facies proportion as a function of areal location (x,y) and are denoted as P^k_a (x,y). These three types of proportions can be obtained through a combination of well and seismic data.

The vertical proportion curve and areal proportion map have implicit global proportions that may be either inconsistent with each other or the reference global proportion; therefore, they are rescaled accordingly:

$$P_v^k(z) = p_v^k(z)\left(\frac{P_g^k}{\int_0^1 p_v^k(z)dz}\right) \tag{26}$$

$$P_a^k(z) = p_a^k(z)\left(\frac{P_g^k}{\int_0^{x_{max}} \int_0^{y_{max}} p_a^k(x,y)dydx}\right) \tag{27}$$

where x_{max} and y_{max} are the areal limits to the reservoir layer in the x_2 and y_2 coordinate system, see Table 1.

Probabilistic/Stratigraphic Specification of a Geologic Parameter

Two characteristics of the geological/geometrical parameters required for modeling are that (1) each parameter may take a range of possible values according to a probability distribution, and (2) the range of values changes with the stratigraphic position/time z. Therefore, the following geological inputs will be specified with a series of conditional distributions for a discrete set of z values between the stratigraphic base (z=0) and the stratigraphic top (z=1), e.g., F(g|(z)) for the cdf of parameter g given stratigraphic position z. Figure 12 illustrates how the quantile values could change with time or z level.

Channel Complex and Channel Geometry

The following input distributions are required to specify the channel complex geometry, (1) angles α (see Fig. 3), (2) departure from channel complex direction $f^{cc}(y_3)$ (see Figure 4) and correlation length in the y_3 direction, (3) thickness, (4) width-to-thickness ratio, and (5) net-to-gross ratio within the channel complex.

A greater number of parameters are required to specify the channel geometry because the thickness and width of each channel is not constant: (1) departure from channel complex direction $f^c(y_3)$ (see Fig. 7) and correlation length in the y_3 direction, (2) average thickness, (3) thickness undulation and correlation length of thickness undulation, (4) width-to-thickness ratio, (5) width undulation and correlation length of width undulation, and (6) channel base roughness.

Well Data

The facies, porosity, and permeability values are known along each well; non-cored wells may only have facies and porosity data. At some fine level of resolution (say, each decimeter along a well) the well data may be recorded at each of n intervals as $f(\mathbf{u}_i)$, $\phi(\mathbf{u}_i)$, $k(\mathbf{u}_i)$,i=1,...,n, where f is a categorical variable giving the facies, ϕ is the porosity expressed as a fraction, k is the permeability in milliDarcies, the n data may come from any arbitrary number of wells, and the location vectors $\mathbf{u}_i$,i=1,...,n may be arbitrarily set to the x_2, y_2, z_2 coordinate system for modeling a specific reservoir layer. Recall that all coordinate conversions are reversible; therefore, knowing the locations of the well data in one set of coordinates provides non-equivocal knowledge in all coordinate systems.

Simulation Procedure

Each reservoir layer is modeled independently and then merged with other layers according to appropriate erosion and truncation rules. For a given layer, all data are converted to the x_2, y_2, z_2 coordinate system, see Table 1. All of the geologic inputs described above must be specified prior to modeling. We expect that many of these parameters will be difficult to infer from available data. Some parameters, such as width-to-thickness ratios, may be kept constant at some realistic value, say 50:1 (real distance units). Sensitivity studies can be considered on other parameters to judge the importance and to assess the visual acceptability of the resulting realizations.

The simulation procedure is sequential or hierarchical. First, the channel complex distribution is established. Second, the distribution of channels within each channel complex. Third, the porosity is assigned using appropriate channel coordinates. Finally, the permeability is assigned conditional to the facies and porosity. Only the first two steps will be described here since conventional algorithms can be used for porosity and permeability modeling[11].

Conditioning to the facies succession along wells and to facies proportion data is accomplished via an objective function that measures mismatch from the known facies at wells and proportion curves and maps. At each stage of simulation an iterative procedure is used to perturb the set of channel complexes or channels until an acceptably low objective function is obtained[12].

For notation, the * is used to identify quantities from a stochastic realization and the absence of a * will identify reference or target quantities, e.g., $P^k_v(z)$ is the reference proportion of facies k at level z and $P^{k^*}_v(z)$ is the actual proportion of facies k at level z in a realization.

Channel Complex Simulation

Each channel complex is a volume within which a number of channels will ultimately be placed. The indicator variable

$$i_{cc}(\mathbf{u}) = \begin{cases} 1, & \text{if } \mathbf{u} \text{ is within a channel complex} \\ 0, & \text{otherwise} \end{cases} \tag{28}$$

defines whether a channel complex is present or absent at any location $\mathbf{u}$. Knowing the number of channel complexes and their geometric parameters it is possible to define $i_{cc}(\mathbf{u})$ for all locations in the area of interest. The presence of a channel complex does not necessarily imply the presence of a channel. A channel complex has a net-to-gross ratio (proportion of channel facies) less than 1.0. The proportion of channel facies at each location, $p_{cc}(\mathbf{u})$, is zero outside of a channel complex and defined from the channel complex net-to-gross ratio when in a channel complex. When two channel complexes overlap at location $\mathbf{u}$ the one with the higher stratigraphic position z takes precedence.

The distribution of channel complexes should honor well data and coarse-scale facies proportions. At this coarse scale, there are two constraints due to well data, (1) a channel complex must be present where a channel is intersected by a well, and (2) a channel complex should not be present at long (defined by the size of the channel complexes) intersections of non-channel facies. To quantify the first constraint another indicator variable is defined for all well intersections:

$$i_w(u_i) = \begin{cases} 1, & \text{if } \mathbf{u} \text{ is within a channel} \\ 0, & \text{otherwise} \end{cases} \tag{29}$$

A second well-based indicator variable will be defined to flag those locations that are surely outside of a channel complex:

$$j_w(\mathbf{u}_i) = \begin{cases} 1, & \text{if } \mathbf{u}_i \text{ is within distance } d_{\max} \text{ of a location } \mathbf{u}_l, l = 1,\dots,n \text{ where } i(\mathbf{u}_l) = 1 \\ 0, & \textit{otherwise} \end{cases} \tag{30}$$

The magnitude of the distance d_{max} is on the order of the size of a channel complex, e.g., it could be set to the average channel complex size.

Now, the objective function for channel complex simulation could contain five components relating to facies proportions and well data:

$$\begin{aligned} O_{cc} = {} & \omega_1 \sum_{k=1}^{K} \left[P_g^k - P_g^{k*} \right]^2 + \omega_2 \sum_{k=1}^{K} \sum_{z=1}^{N_z} \left[P_v^k(z) - P_v^{k*}(z) \right]^2 \\ & + \omega_3 \sum_{k=1}^{K} \sum_{x}^{N_x} \sum_{y=1}^{N_y} \left[P_a^k(x,y) - P_a^{k*}(x,y) \right]^2 \\ & + \omega_4 \sum_{i:i_w(\mathbf{u}_i)=1} \left[i_w(\mathbf{u}_i) - i_{cc}(\mathbf{u}_i) \right]^2 \\ & + \omega_5 \sum_{i:j_w(\mathbf{u}_i)=1} \left[j_w(\mathbf{u}_i) - i_{cc}(\mathbf{u}_i) \right]^2 \end{aligned} \tag{31}$$

where ω_i is a weight to objective function component i. These weights are automatically determined such that each component has, approximately, equal importance[8]. Estimates of the proportions $P^{k^*}_g$, $P^{k^*}_v(z)$, and $P^{k^*}_a(x,y)$ are calculated from $p_{cc}(\mathbf{u})$.

The goal at this stage of simulation is to establish the K channel complexes and their geometric attributes. This is done in an iterative fashion:

1. Start with no channel complex: K=0, that is, empty arrays $i_{cc}(\mathbf{u})=0, \forall\, \mathbf{u} \in A$, and $p_{cc}(\mathbf{u})=0.0, \forall\, \mathbf{u} \in A$.
2. Define an array of operations: *add*, *remove*, *translate*, and *rotate*. Randomly choose one operation from this array and perform the operation. Initially, channel complexes will be added.
3. Update the objective function O_{CC} and decide the

acceptance or rejection of that operation according to the decision rule (could use a simulated annealing schedule or some other scheme[8]). If needed, update the list of channel complexes, the $i_{cc}(\mathbf{u})$ variable, and the $p_{cc}(\mathbf{u})$ variable.

4. Return to step 2 until O_{CC} is deemed low enough.

The parameters for each channel complex are drawn from the geological/geometrical input distributions; therefore, the size and shape distributions are honored in the final realization.

When the simulation is finished the list of channel complexes and their parameters, a raster image of the $i_{cc}(\mathbf{u})$ and $p_{cc}(\mathbf{u})$ variables, and summaries of data conditioning could be reported.

Channel Simulation

A new indicator variable

$$i_c(\mathbf{u}) = \begin{cases} 1, \text{if } \mathbf{u} \text{ is within a channel} \\ 0, \text{otherwise} \end{cases} \quad (32)$$

defines whether a channel is present or absent at any location **u**. This indicator variable can be retrieved everywhere in the model by the geometric description of all channels.

The distribution of channels should honor well data and facies proportions. At this final finer scale, there is a single constraint due to well data: a channel must be present where a channel is intersected by a well and a channel should not be present where a channel is not intersected by a well. The $i_w(\mathbf{u}_i), i=1,\dots,n$ indicator variable defined above will be considered.

The objective function for channel simulation could contain four components relating to facies proportions and well data:

$$\begin{aligned} O_c = {} & \omega_1 \sum_{k=1}^{K} \left[P_g^k - P_g^{k*}\right]^2 + \omega_2 \sum_{k=1}^{K} \sum_{z=1}^{N_z} \left[P_v^k(z) - P_v^{k*}(z)\right]^2 \\ & + \omega_3 \sum_{k=1}^{K} \sum_{x}^{N_x} \sum_{y=1}^{N_y} \left[P_a^k(x,y) - P_a^{k*}(x,y)\right]^2 \\ & + \omega_4 \sum_{i:i_w(\mathbf{u}_i)=1} \left[i_w(\mathbf{u}_i) - i_c(\mathbf{u}_i)\right]^2 \end{aligned} \quad (33)$$

where ω_i is a weight to objective function component i. These weights are automatically determined such that each component has, approximately, equal importance[12]. Estimates of the proportions P^{k*}_g, $P^{k*}_v(z)$, and $P^{k*}_a(x,y)$ are calculated from the channel indicator variable $i_c(\mathbf{u})$.

At this stage of simulation the goal is to establish the number $L_k, k=1,\dots,K$ of channels within each channel complex and their geometric attributes. This is done in an iterative fashion:

1. Start with no channels: $L_k=0$, $k=1,\dots,K$ that is, an empty array $i_c(\mathbf{u})=0$, $\forall\, \mathbf{u} \in A$.
2. Define an array of operations: *add*, *remove*, *translate*, and *rotate*. Randomly choose one operation from this array and perform the operation. Initially, channels will be added.
3. Update the objective function O_C and decide the acceptance or rejection of that operation according to the decision rule. If needed, update the list of channels and the $i_c(\mathbf{u})$ variable.
4. Return to step 2 until O_C is deemed low enough.

The parameters for each channel are drawn from the geological/geometrical input distributions; therefore, the size and shape distributions are honored in the final realization.

When the simulation is finished the computer program can report the list of channels and their parameters, a raster image of the $i_c(\mathbf{u})$ and summaries of data conditioning.

Porosity / Permeability Simulation

The porosity and permeability within each channel is simulated independently using conventional geostatistical algorithms such as sequential Gaussian simulation, indicator simulation, or annealing-based algorithms. The well data ($\phi(\mathbf{u}_i)$, $k(\mathbf{u}_i)$, $i=1,\dots,n$), transformed to the appropriate x_8, y_3, z_2 coordinate system, are used as conditioning data when they fall within the boundaries of the channel.

HEKLA Example

The Hekla reservoir is a portion of a large North Sea fluvial deposit offshore Norway. The Hekla data set is suitable for demonstrating the algorithm described above. The data set includes 20 wells containing facies and petrophysical properties and seismic data defining reservoir geometry and providing impedance data. Fig. 12 shows two major reservoir layers: H1 on the top and H2 on the bottom. The morphology of the reservoir is largely shaped by two NNE trending normal faults. Five facies are distinguished in well data, conglomerate, channel sand, crevasse sand, crevasse levee, and overbank mudstone. For this particular case study, the first three sand type facies are combined as channel facies and the last two shale type facies are combined as non-channel facies.

The approach is to simulate the two layers independently and then reassemble them into a complete reservoir model.

Input Parameters

Vertical proportion curves for both H1 and H2 are obtained from the 20 wells and are shown on Fig. 13. H1 and H2 have global proportions of channel facies of 40% and 22% respectively. Areal proportion maps of channel facies for both H1 and H2 are obtained by kriging, see Fig. 14. The areal proportion maps suggest a general NNE-trending facies distribution. The H2 areal map shows a trend a few degrees east and a relatively homogeneous facies pattern. The various input parameters for the program FLUVSIM (coded in C to perform modeling as described above) are listed in Table 2 for the H1 layer and Table 3 for the H2 layer.

As much as possible, the input parameters are based on data. Some intelligent guesses of certain parameters is inevitable due to data paucity.

FLUVSIM Realizations

Using input parameters specified in Table 2 and Table 3, ten realizations were generated on a DEC-Alpha machine. The simulation grid size for both layers is 101 by 131 by 20, the four conditioning items, well data, global proportion, vertical proportion, and areal proportion, are weighted equally in the objective function, and the program was terminated as soon as objective function value declines below 10% mismatch. The results for well conditioning data mismatch, global proportion mismatch, vertical proportion mismatch, areal proportion mismatch, and final objective function value are listed in Table 4.

Satisfactory results were generated with reasonable CPU time. One could improve the above numbers by specifying a more demanding stopping objective function value at the cost of more CPU time.

Data conditioning is not evenly achieved with equally weighted objective functions. Well data and the global proportion tend to be honored more easily, whereas vertical and areal proportions contribute more mismatch to the objective function. The reason lies in the nature of the perturbation which is based on objects (channel complexes and channels). For instance, one operation involving removal and addition of a channel may not change the global proportion; however, it may have a noticeable impact on vertical or areal proportion. Experience indicates that as the size of the channel complexes and channels are decreased, conditioning is easier and the program converges quicker.

Fig. 15 shows the reproduction of the vertical proportion curves for the first two realizations. The overall trend of the target proportion curve is closely tracked by the simulated values.

Areal proportion map reproduction of realization number one is shown on Fig. 16. The general pattern of the target map is preserved despite local departure from the target.

Areal and vertical slices through the first realization are shown on Fig. 17 and Fig. 18. The channels are absent on the top because of the vertical proportion constraint. The vertical slices reveal satisfactory conditioning at the well locations.

The Hekla data set demonstrates the applicability of the proposed algorithm. The hierarchical object-based technique coupled with an iterative procedure for data conditioning is an incremental advance over traditional object-based algorithms in accommodating geological conceptual models. The number of parameters to infer and the CPU time for data conditioning have been minimized.

Differences from Previous Work

The primary differences of this work with previous work is (1) the asymmetric non-rectangular channel cross section, (2) the use of the channel curvature to control the geomorphology of the channel, (3) direct conditioning to vertical and areal proportions, (4) conditioning at a hierarchy of scales, and (5) using the channel coordinate system to model porosity and permeability.

Conclusions

Reservoir modeling should proceed in a hierarchical or sequential scheme: (1) independently build multiple equiprobable stochastic reservoir models, (2) independently model each major reservoir layer bounded by chronostratigraphic surfaces, (3) model the distribution of channel complexes to honor well data and perhaps locally varying facies proportions, (4) position channels within each channel complex to honor well data and a more detailed representation of the facies proportions, and then (5) assign porosity and permeability in a coordinate system aligned with the channel coordinates. This can be seen as a hybrid combination of object-based modeling for major geological features and cell-based modeling for porosity and permeability.

An eightfold set of coordinate transformations makes it possible to model geometrically complex fluvial reservoir features. Since each transform is reversible, it is straightforward to reconstruct the model in any coordinate system and to accomplish data conditioning at any level of coordinate transformation. In practice, the distributions of geometric / geologic parameters may be difficult to infer from available reservoir data. It will be necessary to borrow such distributions from outcrops, modern analogues, and densely drilled fields. The geologic input parameters required by this modeling approach are consistent with modern sequence stratigraphic concepts.

The iterative approach to honoring local conditioning data and vertical or areal average facies proportions is computationally efficient. This efficiency is due to the sequential nature of conditioning: the channel complexes are positioned to honor coarse-scale features, channels are then positioned to honor fine-scale facies data, last porosity and permeability are modeled to honor fine-scale porosity and permeability variations.

The hierarchical object-based scheme presented in this paper has been custom designed for braided stream fluvial reservoirs. Similar hierarchical schemes could be custom-tailored to different depositional environments.

Acknowledgements

The financial support of the Stanford Center for Reservoir Forecasting (SCRF) is gratefully acknowledged. The authors would also like to thank Prof. A.G. Journel for helpful suggestions throughout this work including the channel cross section model and the use of stochastic averaging as a fast 1-D simulation algorithm.

Nomenclature

γ	=	variogram function
$\mathbf{h}$	=	lag separation vector
I	=	indicator transform
i	=	indicator transform data value
ϕ	=	porosity
RT	=	rock type (usually based on lithology or facies)
ρ	=	correlation coefficient
$\mathbf{u}$	=	location coordinates vector

References

1. Haldorsen, H.H. and Damsleth, E.: "Stochastic Modeling," *JPT*, April, 1990, pp. 404-412.

2. Alabert, F.G., and Modot, V.: "Stochastic Models of Reservoir Heterogeneity: Impact on Connectivity and Average Permeabilities," paper SPE 24893 presented at the 67th Annual Technical Conference and Exhibition of the SPE, Washington, DC, October 4-7, 1992.

3. Bridge, J., and Leeder, M., (1979), A simulation model of alluvial stratigraphy: Sedimentology, v. 26, p. 617-644.

4. Clemensten, R. and others, (1990), A computer program for evaluation of fluvial reservoirs, *in* Buller and others, eds., North Sea Oil and Gas Reservoirs II: Graham and Trotman, London.

5. Henriquez, A. and others, (1990), Characterization of fluvial sedimentology for reservoir simulation modeling: Society of Petroleum Engineers Formation Evaluation Journal, p. 211-216.

6. Tyler, K., Henriquez, A. and Svanes, T., (1995), Modeling heterogeneities in fluvial domains: a review on the influence on production profile, *in* J.Yarus and R.Chambers, eds., Stochastic Modeling and Geostatistics: Principles, Methods, and Case Studies, American Association of Petroleum Geologists Computer Applications in Geology, no. 3, p. 77-89.

7. Mackey, S., and Bridge, J., (1992), A revised FORTRAN program to simulate alluvial stratigraphy: Computers & Geosciences, v. 18, no. 2. p. 119-181.

8. Bratvold, R., Holden, L., Svanes, T., and Tyler, K., (1994), STORM: Integrated 3D stochastic reservoir modeling tool for geologists and reservoir engineers: Society of Petroleum Engineers Paper number 27563.

9. VanWagoner, J., Mitchum, R., Campion, K., and Rahmanian, V., (1990), Siliciclastic Sequence Stratigraphy in Well Logs, Cores, and Outcrops: Concepts for High-Resolution Correlation of Time Facies: The American Association of Petroleum Geologists, Tulsa, Oklahoma, 55 p.

10. Isaacs, E.H. and Srivastava, R.M.: *An Introduction to Applied Geostatistics*: Oxford University Press, New York, 1989.

11. Deutsch, C., and Journel, A., (1992), GSLIB: Geostatistical Software Library and User's Guide: Oxford University Press, New York, 340 p.

12. Deutsch, C., and Cockerham, P., (1994), Practical considerations in the application of simulated annealing to stochastic simulation: Math. Geology, v. 26, no. 1, p. 67-82.

	Transform	Fig. no.	from X	from Y	from Z	to X	to Y	to Z
1	Vertical Stratigraphic Coordinates		x_1	y_1	z_1	x_1	y_1	z_2
2	Areal Translation and Rotation		x_1	y_1	z_2	x_2	y_2	z_2
3	Channel Complex Translation and Rotation		x_2	y_2	z_2	x_3	y_3	z_2
4	Channel Complex Straightening		x_3	y_3	z_2	x_4	y_3	z_2
5	Relative Channel Complex Coordinate		x_4	y_3	z_2	x_5	y_3	z_2
6	Channel Translation		x_5	y_3	z_2	x_6	y_3	z_2
7	Channel Straightening		x_6	y_3	z_2	x_7	y_3	z_2
8	Relative Channel Coordinate		x_7	y_3	z_2	x_8	y_3	z_2

Table 1: Summary of eight-step coordinate transformations from largest to smallest scale.

Parameter	Channel Complex	Channel
Orientation (triangular distribution, degrees)	20, 30, 40	N/A
Width (triangular distribution, meters)	500, 750, 1000	50,250, 500
Width/Height Ratio (triangular distribution)	2, 6, 10	5, 15, 25
Departure and Correlation Length (meters, meters)	500,3000	50, 200
Global Proportion	0.40	0.40
Net-to-Gross ((triangular distribution)	0.5, 0.7, 0.9	N/A
Vertical Proportion	see figure	see figure
Areal Proportion	see figure	see figure

Table 2: Summary of input parameters for H1 layer.

Parameter	Channel Complex	Channel
Orientation (triangular distribution, degrees)	22, 35, 45	N/A
Width (triangular distribution, meters)	500, 750, 1000	50,250, 500
Width/Height Ratio (triangular distribution)	2, 6, 10	5, 15, 25
Departure and Correlation Length (meters, meters)	500,3000	50, 200
Global Proportion	0.40	0.40
Net-to-Gross ((triangular distribution)	0.5, 0.7, 0.9	N/A
Vertical Proportion	see figure	see figure
Areal Proportion	see figure	see figure

Table 3: Summary of input parameters for H2 layer.

Realization	Well	Global Prop.	Vertical Prop.	Areal Prop.	CPU (sec)	Obj. Val. %
1	8.2	5.0	10.9	11.2	487.3	8.82
2	5.1	3.6	15.0	13.7	518.2	9.35
3	9.6	5.7	12.1	9.2	531.8	9.15
4	6.4	4.4	8.0	15.6	498.7	8.6
5	6.1	5.1	10.4	14.9	556.2	9.12
6	8.9	6.8	12.3	12.1	518.4	9.95
7	7.9	4.1	11.7	11.3	498.9	8.75
8	5.0	6.1	13.1	13.4	503.1	9.4
9	7.3	5.5	9.7	11.8	526.2	8.58
10	5.1	4.6	11.2	12.7	518.5	8.40

Table 4: Summary of FLUVSIM results

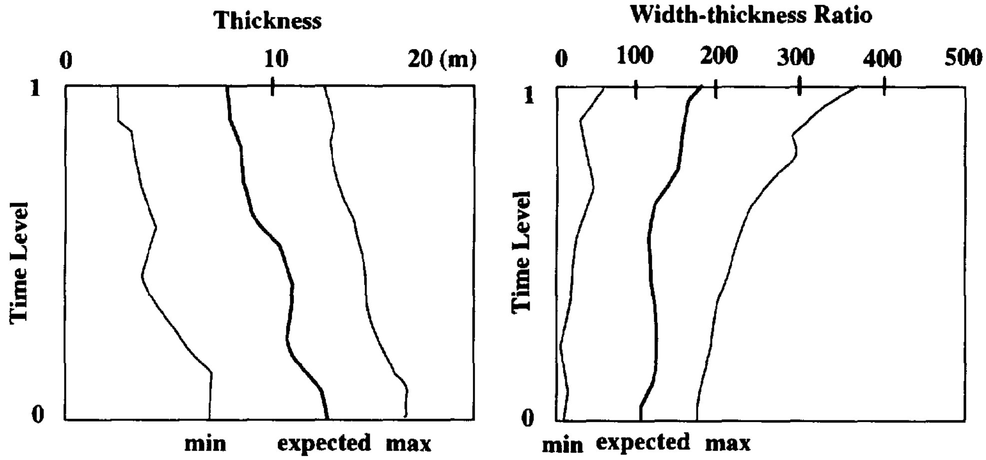

Figure 11: Charts illustrating distributions of channel thickness and width-thickness ratio as a function of time level.

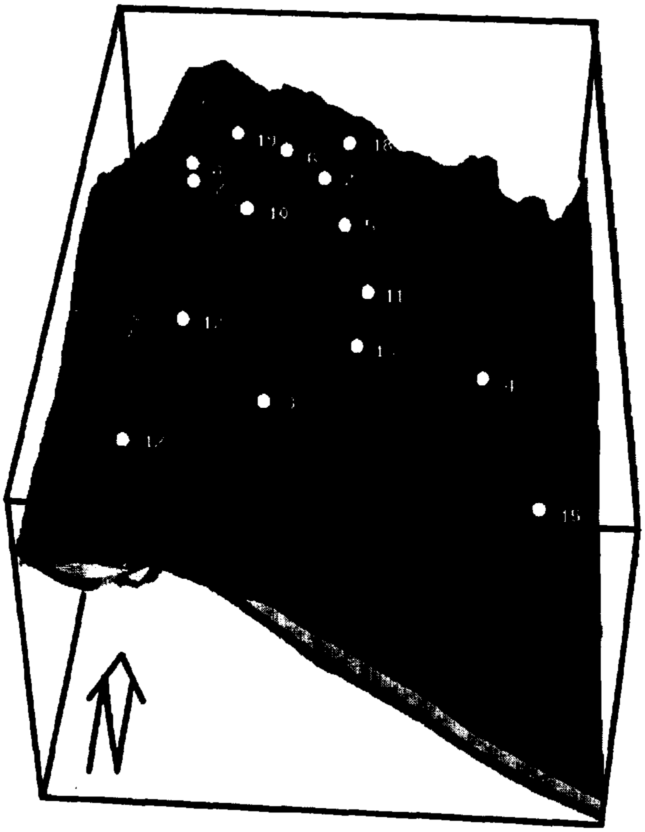

Figure 12: A 3-D view of the Hekla reservoir and its reservoir layers.

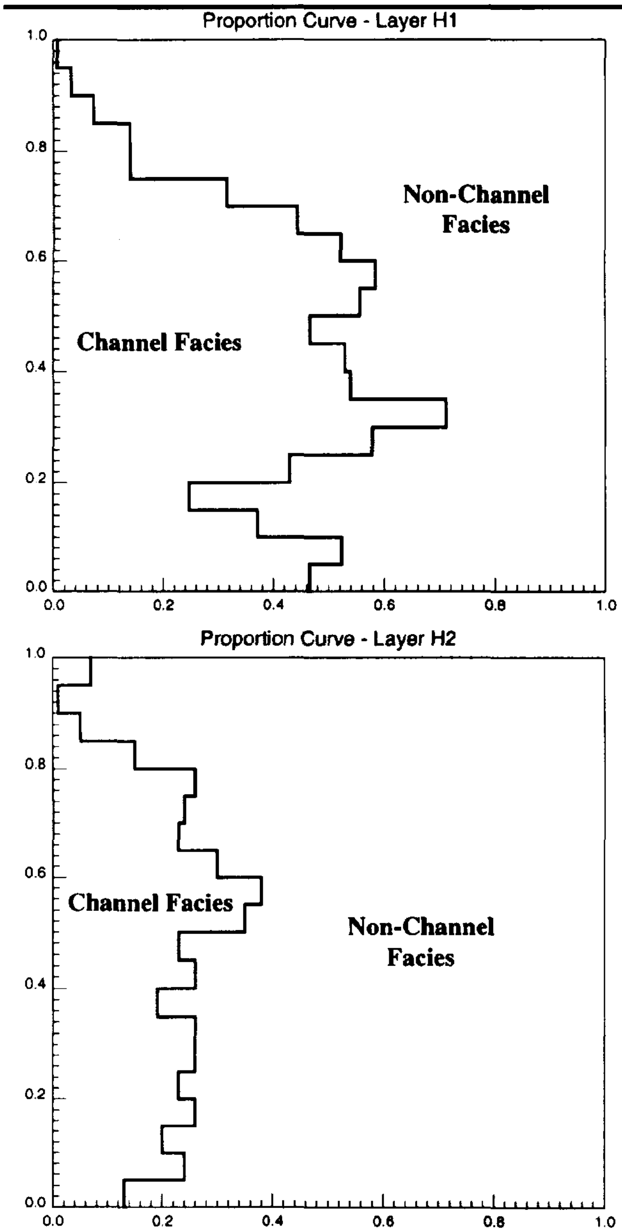

Figure 13: Target vertical proportion curves for H1 and H2 layers.

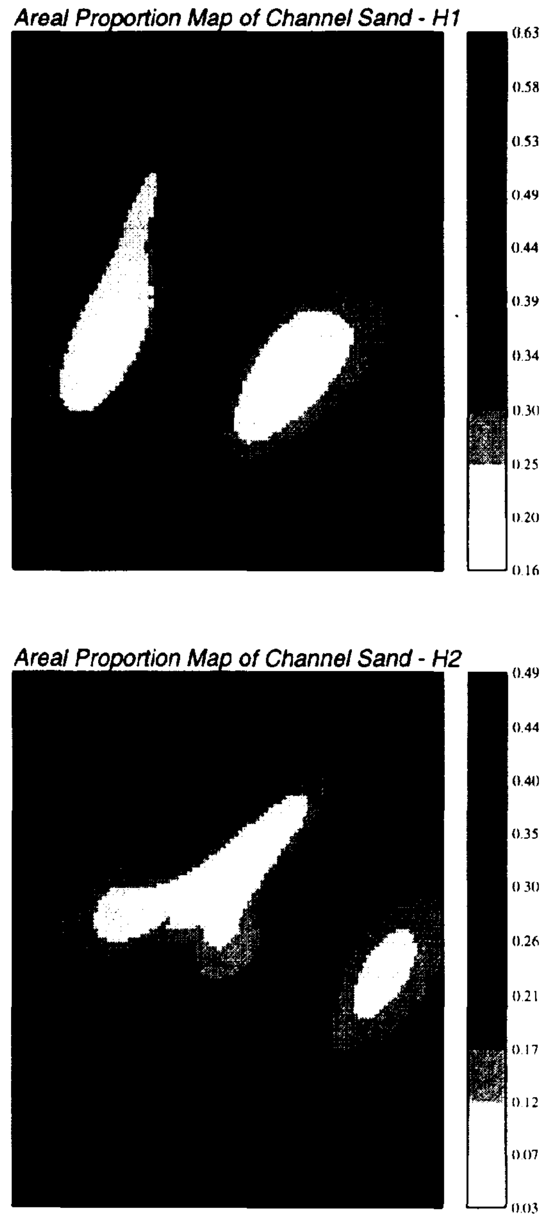

Figure 14: Target areal proportion maps for H1 and H2.

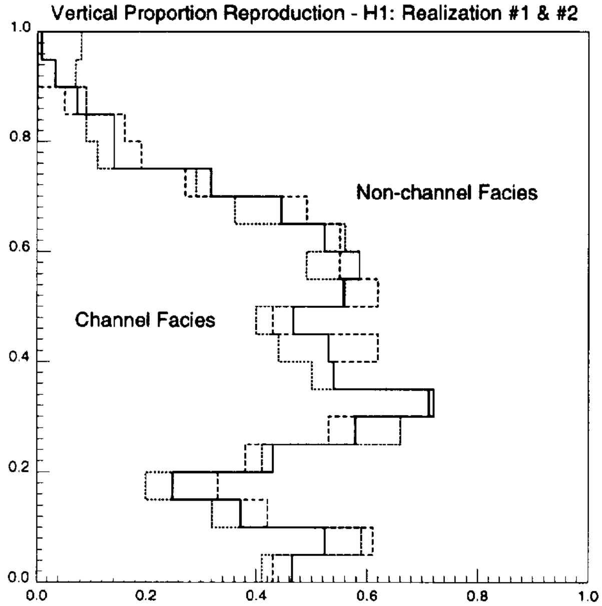

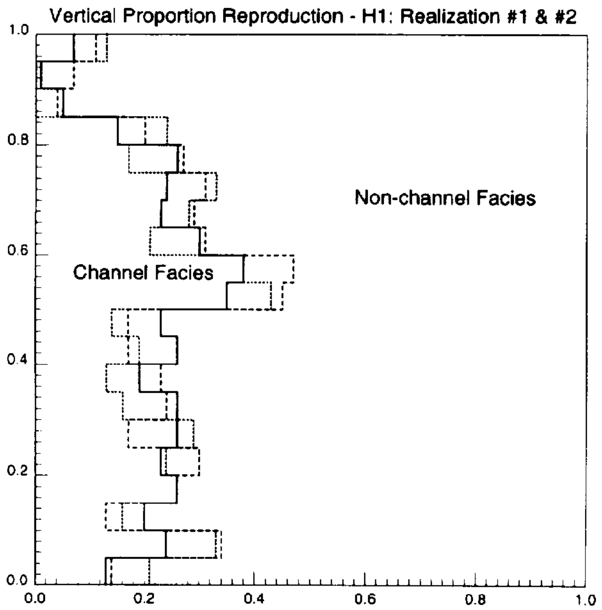

Figure 15: Vertical proportion curves reproduction by the first two realizations. The solid line indicates the input target curve and the dotted and dashed lines represent the two realizations

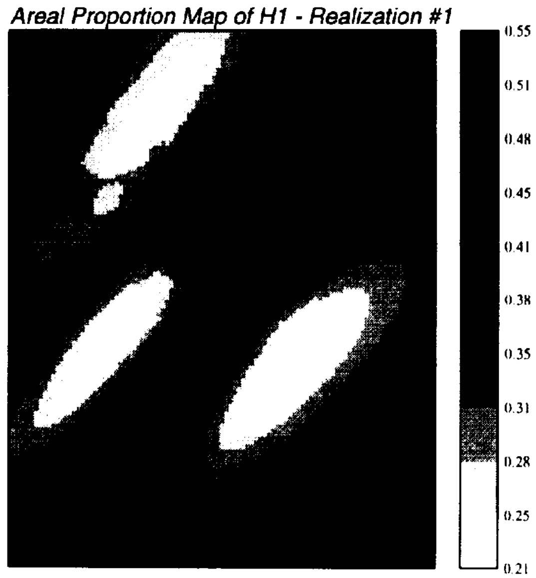

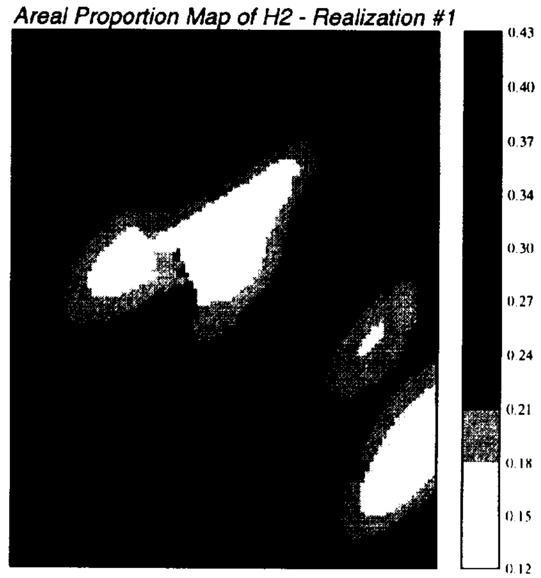

Figure 16: Areal proportion map reproduction by realization number one.

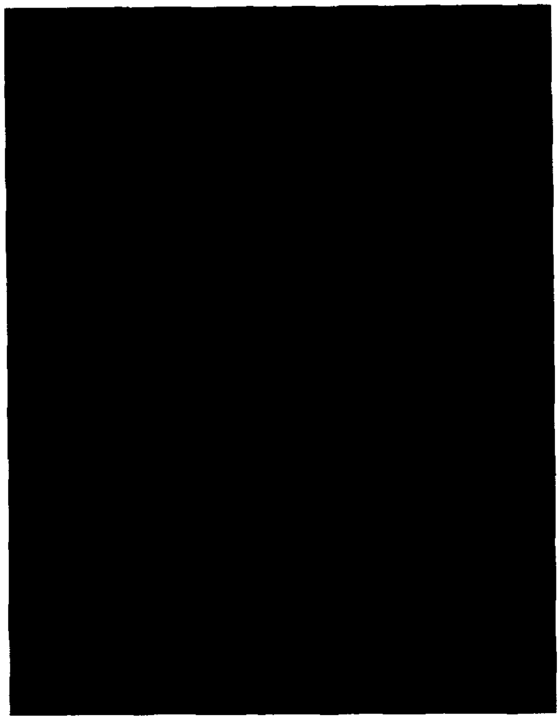

Figure 17: A horizontal slice toward the bottom of the 3-D cube, showing general channel orientation and intercutting.

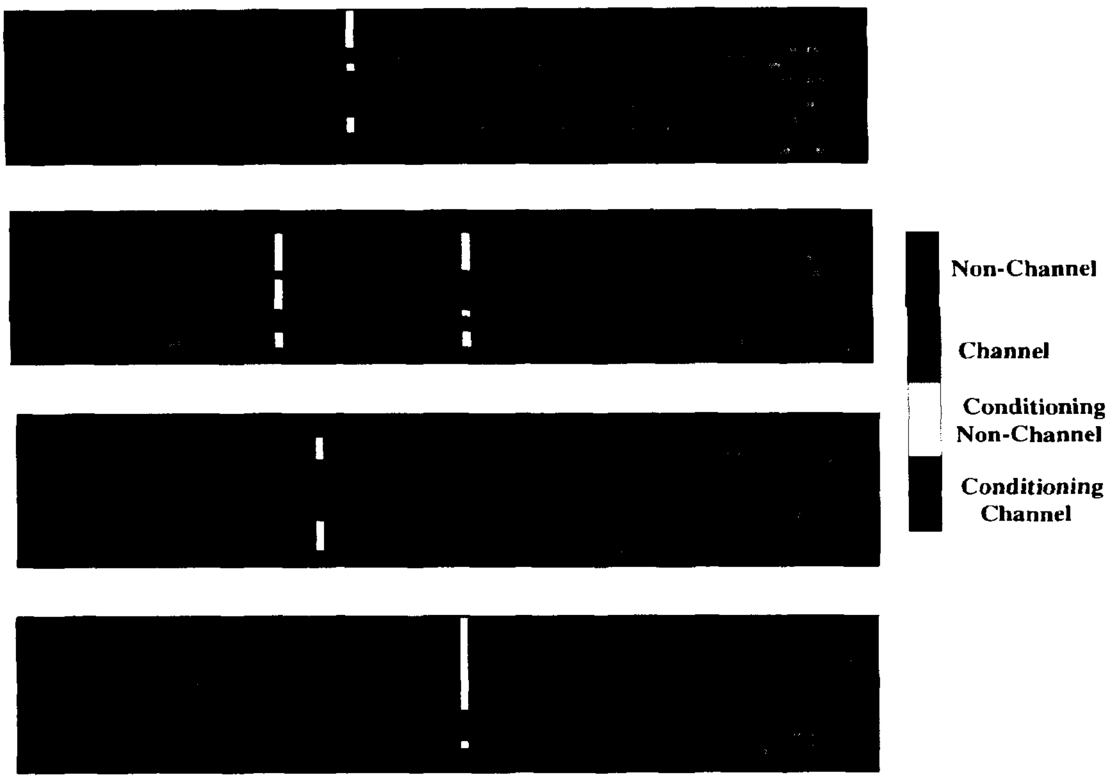

Figure 18: cross sections showing well data and conditioning.